Double acid etching treatment of dental implants for enhanced biological properties

Lluís Giner[1], Montse Mercadé[1], Sergi Torrent[2,3], Miquel Punset[2,3], Román A. Pérez[1], Luis M. Delgado[1], Francisco Javier Gil[1-3]

[1] International University of Catalonia (UIC Barcelona), Barcelona - Spain
[2] Biomaterials, Biomechanics and Tissue Engineering Group, Department of Materials Science and Metallurgy, ETSEIB, Technical University of Catalonia (UPC), Barcelona - Spain
[3] Research Centre in NanoEngineering (CrNE), UPC, Barcelona - Spain

ABSTRACT

Background: The topographical features on the surface of dental implants have been considered as a critical parameter for enhancing the osseointegration of implants. In this work, we proposed a surface obtained by a combination of shot blasting and double acid etching. The double acid etching was hypothesized to increase the submicron topography and hence further stimulate the biological properties of the titanium implant.
Methods: The topographical features (surface roughness and real surface area), wettability and surface chemical composition were analyzed.
Results: The results showed that the proposed method produced a dual roughness, mainly composed of randomly distributed peaks and valleys with a superimposed nanoroughness, and hence with an increased specific surface area. Despite the fact that the proposed method does not introduce significant chemical changes, this treatment combination slightly increased the amount of titanium available on the surface, reducing potential surface contaminants. Furthermore, the surface showed increased contact angle values demonstrating an enhanced hydrophobicity on the surface. The biological behavior of the implants was then assessed by culturing osteoblast-like cells on the surface, showing enhanced osteoblast adhesion, proliferation and differentiation on the novel surface.
Conclusions: Based on these results, the described surface with dual roughness obtained by double acid etching may be a novel route to obtain key features on the surface to enhance the osseointegration of the implant. Our approach is a simple method to obtain a dual roughness that mimics the bone structure modified by osteoclasts and increases surface area, which enhances osseointegration of dental implants.

Keywords: Acid etching, Osteoblast differentiation, Titanium, Surface topography, Wettability

Introduction

The success of titanium dental implants 5-10 years after implantation depends on the surgical procedure, host bone quality, load distribution and implant material and design, as well as the surface properties (1-3). Among the different

Corresponding authors:
Dr. Lluís Giner
School of Dentistry
Universitat Internacional de Catalunya
08195 Barcelona, Spain
lginer@uic.es

Dr. Francisco Javier Gil
School of Dentistry
Universitat Internacional de Catalunya
08017 Barcelona, Spain
xavier.gil@uic.es

variables, surface features are one of the most important factors, including physicochemical and topographical properties. Previous studies have shown that the modulation of the surface properties has enhanced the osseointegration of dental implants in the short and long term (4-7). In this sense, many studies suggest that microstructured and nanostructured topographies may better guide cell behavior compared with surface chemistry (8).

Nowadays, most commercially available dental implants are manufactured using standard metal machining followed by shot blasting (9), acid or alkaline etching (10), electrochemical treatments (11, 12), plasma spray (13) or a combination of these technologies. All of these technologies attempt to improve the secondary stability of the dental implants, increasing the amount of bone in direct contact with the surface, minimizing the connective tissue formation at this interface (14-16). The increase of bone in direct contact with the surface is more beneficial for the mechanical load transfer to the surrounding bone hard tissue, resulting in a reduction of bone resorption around the dental implants in long-term implantation (17).

In this sense, shot blasting for increasing the roughness amplitude of implant surface stands out as a versatile approach to increase cell adhesion, proliferation and differentiation (18-20). In combination with shot blasting, acid etching has been shown to introduce an overlapped roughness in the nanometer to submicron range, which can be tailored for experimental parameters (21).

In this work we proposed a new surface obtained by shot blasting followed by double acid etching. This double acid etching attempts to increase the overlapped nanoroughness and to create submicron and nanometer scale cavities that mimic the bone structure modified by osteoclasts in order to enhance osseointegration (22-24). Compared with single acid etching, second acid etching is intended to increase the nanoroughness and specific surface area (Fig. 1), which will in turn increase protein adsorption, ultimately modulating cell signaling (23). Further, the influence of this combined surface treatment was assessed in terms of surface topography (morphology and roughness), physicochemical properties (wettability and surface chemical composition) and osteoblast cell response (cell adhesion, proliferation and differentiation).

Materials and methods

Materials

The surface studied (commercially available as Oxigenna) was manufactured and kindly donated by Oxtein Iberia SL. Briefly, an 8-mm-diameter grade II pure titanium bar was machined into 2-mm-thick discs. The discs were then submitted to a shot blasting and double acid etching process, the parameters for which are proprietary to Oxtein Iberia SL. Basically, discs were shot blasted with 160- to 250-μm alumina particles and then etched with hydrofluoric acid at room temperature initially, followed by a further etching step with a mixture containing sulfuric acid. All disks were then rinsed in water and plasma cleaned with argon to remove any potential by-products. These discs were referred to as textured discs, and the as-machined discs were used as the control group. All disks were individually packed and sterilized by gamma-irradiation at 25 kGy and stored until use.

Surface morphology and roughness

A minimum of 5 different samples for each group were used to analyze the surface morphology and roughness. Initially, surface morphology was analyzed under scanning electron microscopy (SEM; Zeiss Neon40 FE-SEM; Zeiss, Germany). White light interferometer microscopy in vertical scanning mode (Optical Profiling System, Wyko NT9300; Veeco Instruments, USA) was used for the roughness evaluation. Data analysis was performed with Wyko Vision 4.10 software (Veeco Instruments, USA), using the standard Gaussian filters provided by Vision software using a cutoff of 0.8 mm, as previously published (9, 20), to discern the sample inclination from the surface roughness. The results allowed the characterization of the average roughness (Sa), root mean squared roughness (Sq), the difference between the average of the 5 highest and 5 lowest points (Sz) and the surface area index
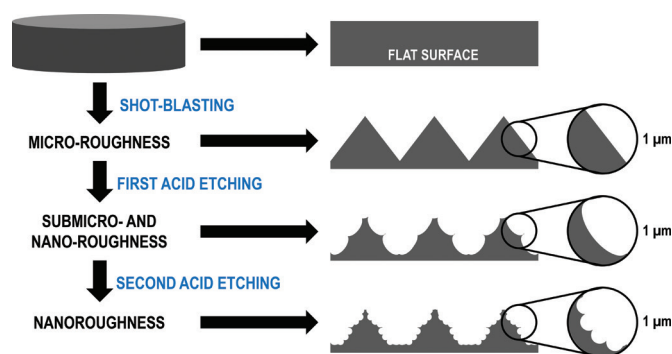

Fig. 1 - Effect of each treatment step (shot blasting, first acid etching and second acid etching) on microroughness and nanoroughness.

(SAI), which is the ratio between the real surface area and the geometric surface area.

Surface wettability

The apparent static contact angle (CA) of a polar liquid (deionized Milli-Q grade water) and a nonpolar liquid (diiodomethane) were measured with the sessile drop method. The measurements were repeated with 10 different samples per group with a constant drop volume of 3 μL. The wettability studies were performed with a video contact angle system (Contact Angle System OCA15plus; Dataphysics, Germany) and analyzed with SCA20 software (Dataphysics, Germany). Due to the interference of surface roughness on the contact angle measurements, the Wenzel equation was used to account for the surface roughness effect (25): $\cos(CA0) = rIA*\cos(CA)$, where CA0 is the apparent (measured) contact angle, rIA is the index area measured by white light interferometry and CA is the intrinsic contact angle.

X-ray photoelectron spectroscopy analysis

Titanium surfaces were analyzed by X-ray photoelectron spectroscopy (XPS) using an XR 50 anode, operating at 300 W, and a Phoibos 150 MCD-9 detector (D8 Advance; SPECS Surface Nano Analysis GmbH, Berlin, Germany). The incidence angle of the beam was 45 degrees, with a detector pass energy of 25 eV with 0.1 eV steps at a pressure below 7.5×10^{-9} mbar. Three samples were studied for each working condition. Casa XPS software (Version 2.3.16; Casa Software Ltd., UK) was used for peak fitting and integration. All binding energies were referenced to the C1s signal with an energy of 284.8 eV.

Cell culture and seeding

Human osteosarcoma osteoblast-like cell line (SaOs-2 [HTB-85]; ATCC, USA) was used for the in vitro cell analysis. Cells were cultured in McCoy's medium supplemented with 10% fetal bovine serum (FBS), 2 mM L-glutamine and penicillin/streptomycin (50 U/mL and 50 μg/mL, respectively) (all reagents from Invitrogen, USA) at 37°C and 5% CO_2 in a humidified incubator. Medium was replaced every other day. Cells were trypsinized when 80% confluence was reached and seeded on titanium discs in triplicates at a density of 12,500
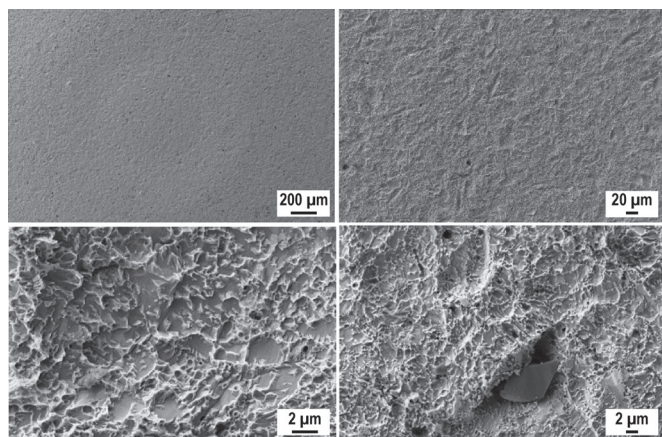
Fig. 2 - Scanning electron microscopy (SEM) images of the textured surface at different magnifications.

Group	Sa (µm)	Sq (µm)	Sz (µm)	SAI
Control	0.18 ± 0.01	0.22 ± 0.01	2.66 ± 0.57	1.02 ± 0.01
Textured	1.36 ± 0.08*	1.74 ± 0.12*	15.69 ± 2.26*	1.92 ± 0.02*

Fig. 3 - Two-dimensional and 3D images obtained by white light interferometry of the control and textured surfaces. Average roughness (Sa), root mean squared roughness (Sq), difference between the average of the 5 highest and 5 lowest points (Sz) and surface area index (SAI) were calculated for textured and control surfaces. *$p < 0.05$.

cells per sample. A tissue culture polystyrene well was used as internal control for the experiment.
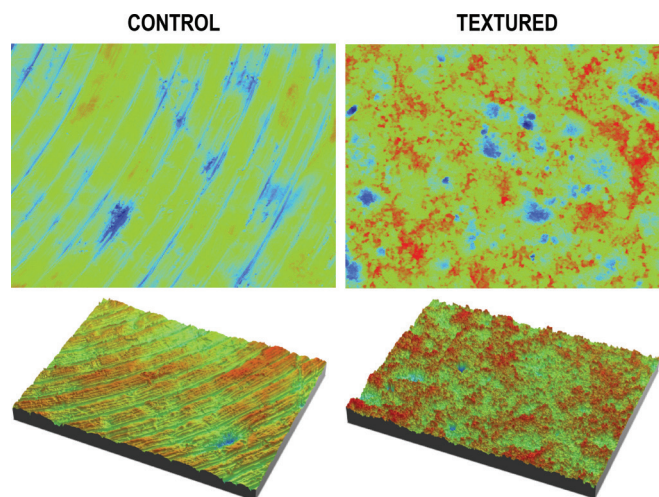
Cell adhesion and proliferation

Cell adhesion was assessed after 6 hours, whereas cell proliferation was assessed after 5 hours, 3 days and 7 days. At each time point, cells were lysed with Mammalian Protein Extraction Reagent (Pierce, USA). Cells on the surfaces studied were determined using the Cytotoxicity Detection Kit LDH (Roche Applied Science, Switzerland) following the manufacturer's guidelines. Briefly, cell lysates were incubated with the reaction solution to allow the catalysis from tetrazolium salt (yellow) to formazan salt (red). The amount of formed formazan salt directly correlates with the quantity of lactate dehydrogenase (LDH) and can be measured using a spectrophotometer at 492 nm (PowerWave HT; BioTek Instruments, Inc., USA). A standard curve was constructed using different cell numbers ranging from 2×10^3 to 40×10^3 cells to correlate the absorbance values with cell number.

Cell differentiation

The lysed cells used to quantify the proliferation were also used to determine alkaline phosphatase (ALP) activity using the SensoLyte pNPP Alkaline Phosphatase Assay Kit (AnaSpec Inc., USA). Each lysate was incubated with p-nitrophenyl phosphate (pNPP) substrate at 37°C for 30 minutes. ALP catalyzes the dephosphorylation of pNNP, which gives rise to a yellow solution. Absorbance was then measured in a microplate reader at 405 nm (PowerWave HT). A calibration curve was prepared using purified ALP from the kit ranging from 0 to 200 ng/mL. Results were normalized versus cell number and incubation time.

Statistical analysis

Numerical data are expressed as means ± standard deviation. Statistical analysis was performed using MINITAB® (version 16.2; Minitab Inc., USA). One-way analysis of variance (ANOVA) followed by Fisher's least significant difference post

hoc test was employed after confirming normal distribution from each sample population (Anderson-Darling normality test) and the equality of variances (Bartlett's and Levene's tests for homogeneity of variance). Nonparametric statistics were used when either or both of the above assumptions were violated, and in those cases, the Mann-Whitney test was carried out. Statistical significance was accepted at a p value of <0.05.

Results

Physicochemical characterization

The textured surface was produced by combining shot blasting and double acid etching. SEM analysis demonstrated that the textured surfaces were composed of peaks and valleys of different sizes, which were randomly distributed with submicron porous structures that were superimposed on the microroughness (Figs. 2 and 3). Additionally, the combined surface treatment induced cavities similar to those created by osteoclasts during bone resorption (Howship's lacunae) (26). As with other shot-blasted surfaces, few alumina particles from the shot blasting remain on the surface after the double acid etching (Fig. 2). The textured surfaces showed significant differences from the control surfaces, with the latter presenting a flat morphology with the typical circular grooves from the machining process (Fig. 3).

Further, a quantitative analysis of the roughnessvariation was completed by white light interferometer microscopy. The 2 surfaces presented statistically significant differences in terms of roughness parameters (Fig. 3). The textured surfaces showed increases in all of the studied roughness parameters: Sa, Sq, Sz and SAI (p<0.05). Textured surfaces
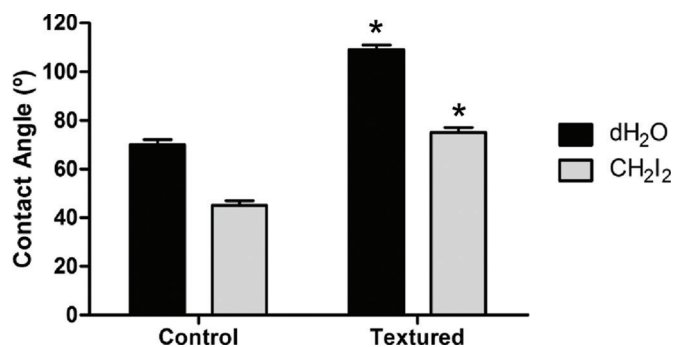
Fig. 4 - Intrinsic contact angles for water (dH_2O) and diiodomethane (CH_2I_2) on textured and control surfaces. *$p<0.05$.

had an increased average roughness (Sa) from 0.18 ± 0.01 μm to 1.36 ± 0.08 μm and surface area index (SAI) from 1.02 ± 0.01 to 1.92 ± 0.02. Regarding the wettability, the textured surfaces had an increased contact angle of water and diiodomethane compared with the control surface ($p<0.05$) (Fig. 4).

XPS analysis revealed the presence of C, O, Ti, Si and N elements on all of the different titanium surfaces (Fig. 5). Although statistical analysis revealed significant differences for C ($p<0.05$), the quantity of C was similar between both conditions (33.1% ± 0.3% C for control vs. 33.9% ± 0.3% C for textured surfaces). Concentration of O was similar for both surfaces ($p>0.05$). Higher amounts of Ti and Al were found on textured surfaces compared with controls ($p<0.05$), while the percentage of Si was significantly reduced for textured surfaces ($p<0.05$). Other elements, such as S, F, Zn and Ca, were found as well in lower amounts (lower than 1%), and none of them showed significant differences between the different surfaces.

Human osteoblast cell response

The adhesion and proliferation of osteoblast-like cell line SaOs-2 was investigated. The number of cells adhered to the textured surface was significantly higher than to the control surfaces ($p<0.05$), inducing a nearly threefold change at 6 hours (Fig. 6). Regarding cell proliferation (Fig. 6), although cells cultured on textured and control surfaces both supported cell proliferation within the initial 3 days, there were no significant differences in cell number ($p>0.05$). At day 7, cell number on the textured surfaces was significantly greater compared with that on control surfaces ($p<0.05$). Cell differentiation was measured through the cell expression of ALP (Fig. 6), an early osteoblastic differentiation marker. The amount of ALP increased over time for textured surfaces, while the values did not increase for the control surfaces. The textured surfaces expressed higher levels of ALP compared with control surfaces at all time points ($p<0.05$), presenting a sixfold increase at day 7.

Discussion

It is well-known that surface properties such as roughness (27), surface composition (28), wettability (29), surface energy and charge (30) have a crucial role in modulating cell response to biomaterials. Although the specific values are not fixed (20), the fact that surface properties intensely determine the initial protein and cell response is widely accepted (31). While this mainly applies to in vitro scenarios, it is also expected that in vivo enhanced surface area and topographical features may enhance osseointegration in the short and long term (4). The vast majority of commercially available dental implants are manufactured using standard metal machining followed by shot blasting and acid etching with different processing parameters to induce a rough surface at the nanometer to submicron level (31).

To our knowledge, no previous work has described in detail a double acid etching process able to increase the surface area as well as other topographical features. This study combined 2 acid etching steps with different purposes: first etching with hydrofluoric acid to generate the microroughness and a second etching with sulfuric acid to obtain the nanoroughness. Moreover, gas plasma was applied to remove any by-products and any potential contaminants from the surface. Above all, this is the first paper that describes 2 different acid etching steps followed by gas plasma treatment. Therefore, we assessed the physical and biological properties of this novel surface; textured samples presented a microroughness composed of peaks and valleys randomly distributed throughout the surface with an average roughness (Sa) of 1.36 ± 0.08 μm.This microroughness involved a superimposed skeletal roughness at the nanometer and submicron scale obtained by the acid etching, which increased the SAI from 1.02 ± 0.01 for the control sample, to 1.92 ± 0.02 for the textured samples. This increase of surface area was higher than that for other surfaces that were measured using the same methodology (20). We also observed some remnants of incrusted aluminium oxide particles on surface, corresponding to residue from the shot blasting which had not been removed by the chemical application. This feature is common in this type of surface process for dental implants (32) and does not interfere with the biological activity of the surface (33).

Overall, the textured surfaces decreased surface wettability with water and diiodomethane – i.e., the process increased the contact angle. This is consistent with a previous publication that showed this effect was more pronounced for surfaces that were shot blasted with aluminium oxide particles than for those shot blasted with silicon carbide (20). This reduction of wettability is also associated with a reduction of the surface energy, and in turn, surface energy modulates the protein absorption such as fibronectin (20). Regarding the surface chemical composition, environmental and process by-products have been defined as inhibition factors for the successful osseointegration of implants (34, 35). Our combination of shot blasting, acid etching and final gas plasma cleaning contributed to reducing environmental contaminants such as Si and to increasing the amount of Ti available on the surface.

The amount of carbon detected can be attributed to absorbed organic species, such as adsorbed hydrocarbons and metal-organic species, which are common in the atmosphere (36). The range of carbon elements detected was previously shown to have minimal detrimental effects on the
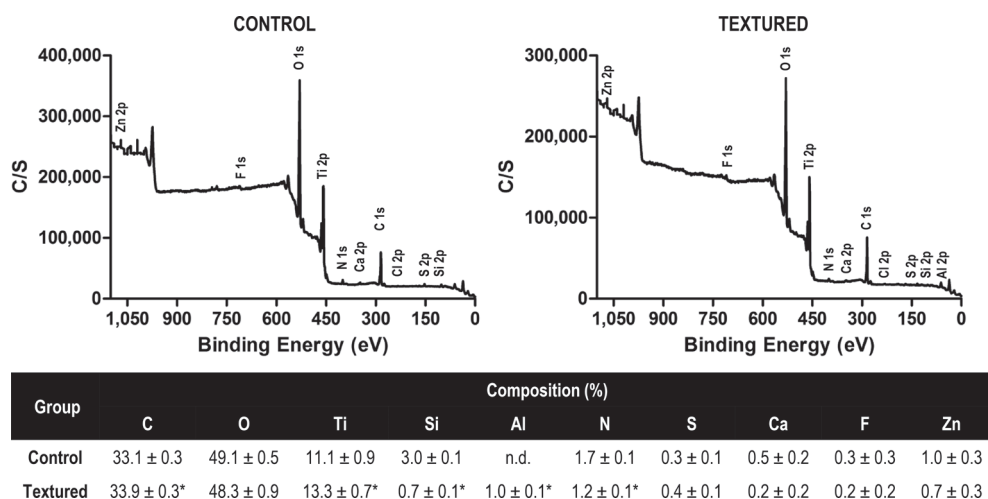
Fig. 5 - Surface chemical composition of the more significant elements on textured and control surfaces: X-ray photoelectron spectroscopy (XPS) survey spectrums, with calculated means and standard deviations. n.d. = nondetectable. *p<0.05.

Group	Composition (%)									
	C	O	Ti	Si	Al	N	S	Ca	F	Zn
Control	33.1 ± 0.3	49.1 ± 0.5	11.1 ± 0.9	3.0 ± 0.1	n.d.	1.7 ± 0.1	0.3 ± 0.1	0.5 ± 0.2	0.3 ± 0.3	1.0 ± 0.3
Textured	33.9 ± 0.3*	48.3 ± 0.9	13.3 ± 0.7*	0.7 ± 0.1*	1.0 ± 0.1*	1.2 ± 0.1*	0.4 ± 0.1	0.2 ± 0.2	0.2 ± 0.2	0.7 ± 0.3

osseointegration of dental implants (34, 37). Consistent with previous publications (15, 38-42), our results showed that textured surfaces improved in vitro osteoblast response, increasing initial cell adhesion, proliferation and differentiation.

Finally, we demonstrated that the textured surface contained potential properties that would support protein adsorption through its wettability characteristics, without inducing any cytotoxic response, while stimulating osteoblast differentiation because of its combined nanoroughness and microroughness. This type of nonpatterned microroughness has been demonstrated to enhance osteoblast proliferation (43). Further studies are required to compare this surface with other available dental implant surfaces, to evaluate other early and late bone differentiation markers (RUNX2, osteocalcin and/or osteopontin) and to study the effect of the nanoroughness in animal models, as Babuska et al have advocated (44). We hypothesize that this textured surface may induce adequate osseointegration in vivo.

Conclusions

In summary, shot blasting of titanium surface followed by double acid etching produced a dual roughness that was composed of peaks and valleys randomly distributed, with a superimposed nanoroughness and increased specific area. Although the textured surface was mainly composed of titanium and oxygen with smaller amounts of surface contaminants such as silicon, it had hydrophobic characteristics that are common in shot-blasted titanium surfaces. Finally, textured surfaces were demonstrated to enhance osteoblast adhesion, proliferation and differentiation. The current study opens up the possibility of a new type of surface that needs to be further characterized but which presents promising features for clinical applications.
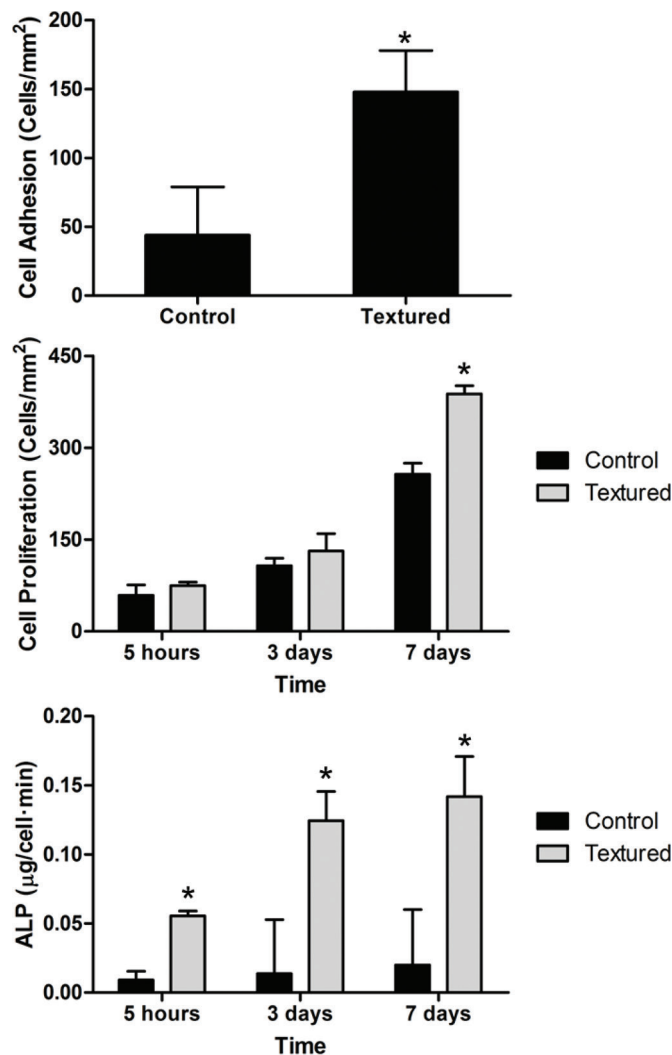
Disclosures

Fig. 6 - Osteoblast adhesion (at 6 hours) and proliferation measured with lactate dehydrogenase (LDH), and differentiation measured with alkaline phosphatase (ALP). *p<0.05.

References

1. Albrektsson T, Brånemark PI, Hansson HA, Lindström J. Os-seointegrated titanium implants: requirements for ensuring a long-lasting, direct bone-to-implant anchorage in man. Acta Orthop Scand. 1981;52(2):155-170.

2. Thomas KA, Cook SD. An evaluation of variables influencing im-plant fixation by direct bone apposition. J Biomed Mater Res. 1985;19(8):875-901.

3. Schwartz-Arad D, Kidron N, Dolev E. A long-term study of im-plants supporting overdentures as a model for implant suc-cess. J Periodontol. 2005;76(9):1431-1435.

4. Le Guéhennec L, Soueidan A, Layrolle P, Amouriq Y. Surface treatments of titanium dental implants for rapid osseointegra-tion. Dent Mater. 2007;23(7):844-854.

5. Fraioli R, Dashnyam K, Kim J-H, et al. Surface guidance of stem cell behavior: chemically tailored co-presentation of integrin-binding peptides stimulates osteogenic differentiation in vitro and bone formation in vivo. Acta Biomater. 2016;43:269-281.

6. Camilo CC, Silveira CA, Faeda RS, de Almeida Rollo JM, Purque-rio BM, Fortulan CA. Bone response to porous alumina implants coated with bioactive materials, observed using different char-acterization techniques. J Appl Biomater Funct Mater. 2017. [Epub ahead of print].

7. Varoni E, Canciani E, Palazzo B, et al. Effect of poly-L-lysine coating on titanium osseointegration: from characterization to in vivo studies. J Oral Implantol. 2015;41(6):626-631.

8. Anselme K, Davidson P, Popa AM, Giazzon M, Liley M, Ploux L. The interaction of cells and bacteria with surfaces structured at the nanometre scale. Acta Biomater. 2010;6(10):3824-3846.

9. Aparicio C, Gil FJ, Fonseca C, Barbosa M, Planell JA. Corrosion behaviour of commercially pure titanium shot blasted with dif-ferent materials and sizes of shot particles for dental implant applications. Biomaterials. 2003;24(2):263-273.

10. Gil FJ, Manzanares N, Badet A, Aparicio C, Ginebra MP. Biomi-metic treatment on dental implants for short-term bone re-generation. Clin Oral Investig. 2014;18(1):59-66.

11. Sul YT, Johansson CB, Röser K, Albrektsson T. Qualitative and quantitative observations of bone tissue reactions to anodised implants. Biomaterials. 2002;23(8):1809-1817.

12. Della Valle C, Rondelli G, Cigada A, Bianchi AE, Chiesa R. A novel silicon-based electrochemical treatment to improve osteoin-tegration of titanium implants. J Appl Biomater Funct Mater. 2013;11(2):e106-e116.

13. Jansen JA, Wolke JG, Swann S, Van der Waerden JP, de Groot K. Application of magnetron sputtering for producing ce-ramic coatings on implant materials. Clin Oral Implants Res. 1993;4(1):28-34.

14. Cochran DL, Nummikoski PV, Higginbottom FL, Hermann JS, Makins SR, Buser D. Evaluation of an endosseous titanium implant with a sandblasted and acid-etched surface in the canine mandible: radiographic results. Clin Oral Implants Res. 1996;7(3):240-252.

15. Aparicio C, Gil FJ, Planell JA, Engel E. Human-osteoblast pro-liferation and differentiation on grit-blasted and bioactive titanium for dental applications. J Mater Sci Mater Med. 2002;13(12):1105-1111.

16. Aparicio C, Padrós A, Gil FJ. In vivo evaluation of micro-rough and bioactive titanium dental implants using histometry and pull-out tests. J Mech Behav Biomed Mater. 2011;4(8):1672-1682.

17. Huiskes R, Ruimerman R, van Lenthe GH, Janssen JD. Effects of mechanical forces on maintenance and adaptation of form in trabecular bone. Nature. 2000;405(6787):704-706.

18. Groessner-Schreiber B, Tuan RS. Enhanced extracellular matrix production and mineralization by osteoblasts cultured on tita-nium surfaces in vitro. J Cell Sci. 1992;101(Pt 1):209-217.

19. Pegueroles M, Aguirre A, Engel E, et al. Effect of blasting treat-ment and Fn coating on MG63 adhesion and differentiation on titanium: a gene expression study using real-time RT-PCR. J Mater Sci Mater Med. 2011;22(3):617-627.

20. Pegueroles M, Aparicio C, Bosio M, et al. Spatial organization of osteoblast fibronectin matrix on titanium surfaces: effects of roughness, chemical heterogeneity and surface energy. Acta Biomater. 2010;6(1):291-301.

21. Schliephake H, Scharnweber D. Chemical and biological func-tionalization of titanium for dental implants. J Mater Chem. 2008;18(21):2404-2414.

22. Puleo DA, Nanci A. Understanding and controlling the bone-implant interface. Biomaterials. 1999;20(23-24):2311-2321.

23. Mendonça G, Mendonça DB, Aragão FJ, Cooper LF. Advancing dental implant surface technology from micron- to nanotopog-raphy. Biomaterials. 2008;29(28):3822-3835.

24. Davies JE, Mendes VC, Ko JC, Ajami E. Topographic scale-range synergy at the functional bone/implant interface. Biomateri-als. 2014;35(1):25-35.

25. Wenzel RN. Resistance of solid surfaces to wetting by water. Ind Eng Chem. 1936;28(8):988-994.

26. Clarke B. Normal bone anatomy and physiology. Clin J Am Soc Nephrol. 2008;3(Suppl 3):S131-S139.

27. Ponsonnet L, Reybier K, Jaffrezic N, et al. Relationship between surface properties (roughness, wettability) of titanium and ti-tanium alloys and cell behaviour. Mater Sci Eng C Mater Biol Appl. 2003;23(4):551-560.

28. Huang Q, Elkhooly TA, Liu X, et al. SaOS-2 cell response to macro-porous boron-incorporated TiO2 coating prepared by micro-arc oxidation on titanium. Mater Sci Eng C Mater Biol Appl. 2016;67:195-204.

29. Sedlaczek J, Lohmann CH, Lotz EM, Hyzy SL, Boyan BD, Schwartz Z. Effects of low-frequency ultrasound treatment of titanium surface roughness on osteoblast phenotype and maturation. Clin Oral Implants Res. 2016.

30. Qiu Q, Sayer M, Kawaja M, Shen X, Davies JE. Attachment, mor-phology, and protein expression of rat marrow stromal cells cultured on charged substrate surfaces. J Biomed Mater Res. 1998;42(1):117-127.

31. Albertini M, Fernandez-Yague M, Lázaro P, et al. Advances in surfaces and osseointegration in implantology: biomi-metic surfaces. Med Oral Patol Oral Cir Bucal. 2015;20(3): e316-e325.

32. Darvell BW, Samman N, Luk WK, Clark RK, Tideman H. Con-tamination of titanium castings by aluminium oxide blasting. J Dent. 1995;23(5):319-322.

33. Naji A, Harmand MF. Cytocompatibility of two coating ma-terials, amorphous alumina and silicon carbide, using hu-man differentiated cell cultures. Biomaterials. 1991;12(7): 690-694.

34. Hayashi R, Ueno T, Migita S, et al. Hydrocarbon deposi-tion attenuates osteoblast activity on titanium. J Dent Res. 2014;93(7):698-703.

35. Bonsignore LA, Goldberg VM, Greenfield EM. Machine oil inhibits the osseointegration of orthopaedic implants by im-pairing osteoblast attachment and spreading. J Orthop Res. 2015;33(7):979-987.

36. Morra M, Cassinelli C, Bruzzone G, et al. Surface chemistry ef-fects of topographic modification of titanium dental implant surfaces: Part 1: surface analysis. Int J Oral Maxillofac Implants. 2003;18(1):40-45.

37. Cassinelli C, Morra M, Bruzzone G, et al. Surface chemistry ef-fects of topographic modification of titanium dental implant surfaces: Part 2: in vitro experiments. Int J Oral Maxillofac Im-plants. 2003;18(1):46-52.

38. Boyan BD, Lohmann CH, Dean DD, Sylvia VL, Cochran DL, Schwartz Z. Mechanisms involved in osteoblast response to implant surface morphology. Annu Rev Mater Res. 2001;31(1):357-371.

39. Anselme K, Bigerelle M, Noel B, et al. Qualitative and quantitative study of human osteoblast adhesion on materials with various surface roughnesses. J Biomed Mater Res. 2000;49(2):155-166.

40. Martin JY, Schwartz Z, Hummert TW, et al. Effect of titanium surface roughness on proliferation, differentiation, and protein synthesis of human osteoblast-like cells (MG63). J Biomed Mater Res. 1995;29(3):389-401.

41. Anselme K, Bigerelle M. Statistical demonstration of the relative effect of surface chemistry and roughness on human osteoblast short-term adhesion. J Mater Sci Mater Med. 2006;17(5):471-479.

42. Zareidoost A, Yousefpour M, Ghaseme B, Amanzadeh A. The relationship of surface roughness and cell response of chemical surface modification of titanium. J Mater Sci Mater Med. 2012;23(6):1479-1488.

43. Anselme K, Bigerelle M, Noël B, Iost A, Hardouin P. Effect of grooved titanium substratum on human osteoblastic cell growth. J Biomed Mater Res. 2002;60(4):529-540.

44. Babuska V, Moztarzadeh O, Kubikova T, Moztarzadeh A, Hrusak D, Tonar Z. Evaluating the osseointegration of nanostructured titanium implants in animal models: current experimental methods and perspectives [review]. Biointerphases. 2016;11(3):030801.